

Publications

12-5-2017

RFID Tags for On- and Off-Metal Applications

Ramiro Augusto Ramirez

Thomas McCrea Weller

Eduardo Antonio Rojas

Follow this and additional works at: <https://commons.erau.edu/publication>



Part of the [Electrical and Electronics Commons](#)

Scholarly Commons Citation

Ramirez, R. A., Weller, T. M., & Rojas, E. A. (2017). RFID Tags for On- and Off-Metal Applications. , (). Retrieved from <https://commons.erau.edu/publication/2182>

This Patent is brought to you for free and open access by Scholarly Commons. It has been accepted for inclusion in Publications by an authorized administrator of Scholarly Commons. For more information, please contact commons@erau.edu.

(12)

United States Patent

Ramirez et al.

(10) Patent No.:

US 9,836,685 B1

(45) Date of Patent:

Dec. 5, 2017

(54) RFID TAGS FOR ON- AND OFF-METAL APPLICATIONS

(71)

Applicants:

Ramiro Augusto Ramirez, Tampa, FL (US); Thomas McCrea Weller, Lutz, FL (US); Eduardo Antonio Rojas, Temple Terrace, FL (US)

(72)

Inventors:

Ramiro Augusto Ramirez, Tampa, FL (US); Thomas McCrea Weller, Lutz, FL (US); Eduardo Antonio Rojas, Temple Terrace, FL (US)

(73)

Assignee:

University of South Florida, Tampa, FL (US)

(*)

Notice:

Subject to any disclaimer, the term of this patent is extended or adjusted under 35 U.S.C. 154(b) by 0 days.

(21)

Appl. No.:

15/215,199

(22)

Filed:

Jul. 20, 2016

(51)

Int. Cl.

G06K 19/04 (2006.01)

G06K 19/077 (2006.01)

G06K 19/00 (2006.01)

(52)

U.S. Cl.

CPC

G06K 19/07722 (2013.01); G06K 19/00 (2013.01); G06K 19/04 (2013.01); G06K 19/07745 (2013.01); G06K 19/07775 (2013.01); G06K 19/07771 (2013.01)

(58)

Field of Classification Search

CPC

G06K 19/07722; G06K 19/07775; G06K 19/07745; G06K 19/07771; G06K 19/00; G06K 19/04; G06K 19/08; H01Q 1/2225; H05K 1/11

USPC

235/488, 487, 492; 340/10.1

See application file for complete search history.

(56) References Cited

U.S. PATENT DOCUMENTS

8,319,694 B2 11/2012 Yang

8,381,998 B1 2/2013 Chang

8,462,073 B2 * 6/2013 Shachar H01P 5/10 29/601

2007/0046548 A1 * 3/2007 Pros H01Q 1/243 343/702

2007/0120677 A1 5/2007 Park

2008/0055045 A1 3/2008 Swan

2008/0111688 A1 5/2008 Nikitin

(Continued)

FOREIGN PATENT DOCUMENTS

WO

2014/057464 A4

4/2014

OTHER PUBLICATIONS

Rao, K. V. S., Sander F. Lam, and Pavel V. Nikitin. "UHF RFID tag for metal containers" Microwave Conference Proceedings (APMC), 2010 Asia-Pacific. IEEE, 2010.

(Continued)

Primary Examiner — Claude J Brown

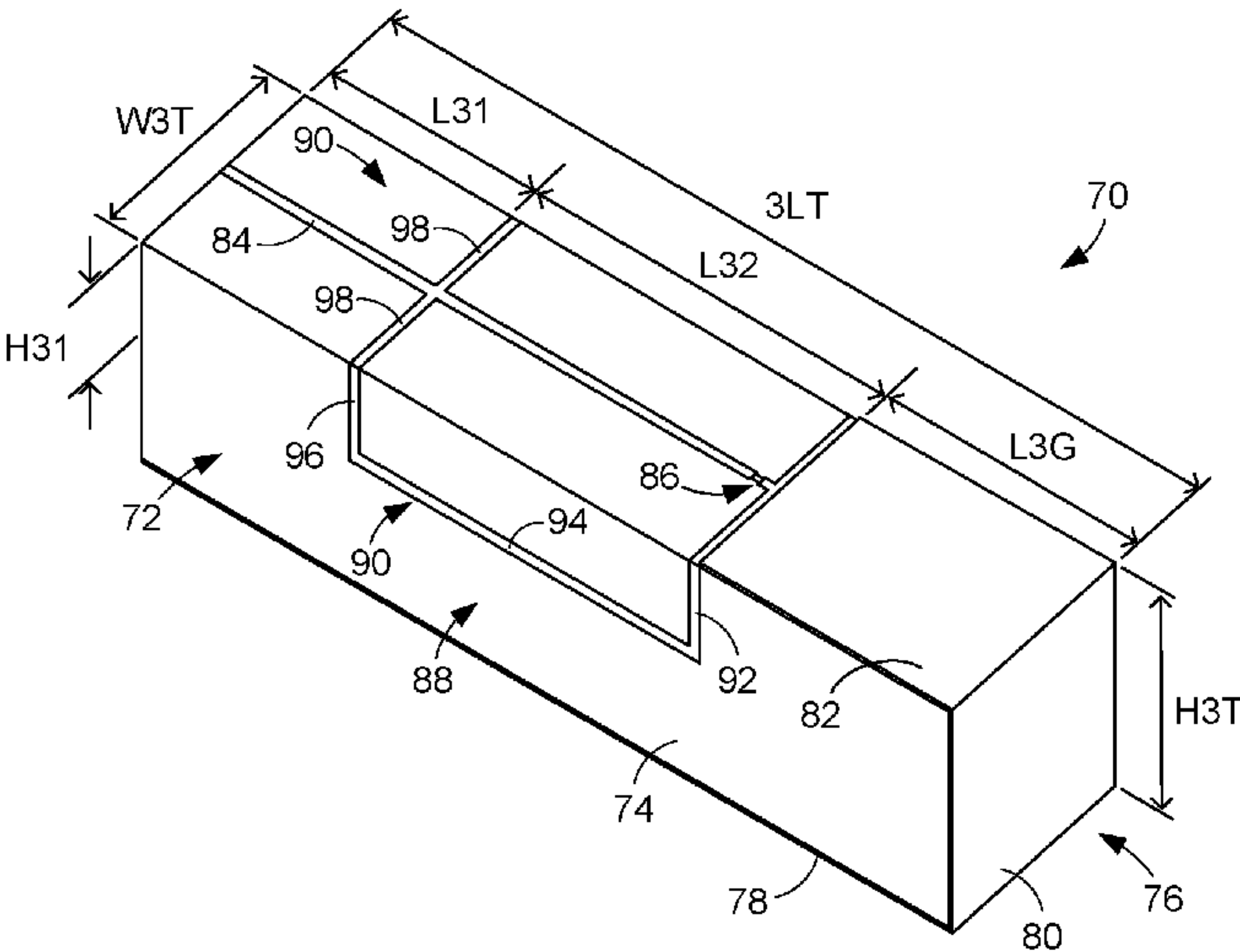
(74) Attorney, Agent, or Firm — Thomas I Horstemeyer, LLP

(57)

ABSTRACT

In one embodiment, a radio-frequency identification (RFID) tag including a substrate having a top surface, bottom surface, opposed end surfaces, and opposed lateral surfaces, a passive RFID integrated circuit (IC) chip mounted to the top surface of the substrate, a monopole antenna that includes a planar radiating arm that extends out from the RFID IC chip along the top surface of the substrate and a matching loop having two grounded matching stubs that surround the chip and a portion of the radiating arm, and a ground plane formed on the bottom surface, an end surface, and the top surface of the substrate, the ground plane being electrically coupled to the matching stubs and the radiating arm.

18 Claims, 9 Drawing Sheets



(56)

References Cited

U.S. PATENT DOCUMENTS

2010/0127943 A1* 5/2010 Inoue H01Q 15/14
343/702
2013/0120197 A1* 5/2013 Lin H01Q 1/38
343/700 MS
2013/0123726 A1* 5/2013 Yu H01Q 1/2225
604/361
2014/0232608 A1* 8/2014 Zhao H01Q 1/38
343/866
2016/0294063 A1* 10/2016 McGough H01Q 9/28

OTHER PUBLICATIONS

Lee, J-W., and B. Lee. "Design of high-Q UHF radio-frequency identification tag antennas for an increased read range." IET micro-waves, antennas & propagation 2.7 (2008): 711-717.
Hodges, Steve, et al. "Assessing and optimizing the range of UHF RFID to enable real-world pervasive computing applications." Pervasive Computing. Springer Berlin Heidelberg, 2007. 280-297.
Hongwei, et al., "3D antenna for UHF RFID tags with near omni-direction", in Antennas, Propagation and EM Theory, 2008; 8th International Symposium.
Ramirez, et al., "3D tag with improved read range for UHF RFID applications using Additive Manufacturing", In Wireless and Micro-wave Technology Conference, 2015 IEEE, 2015.

Phatarachaisakul, et al., "Tag antenna using printed dipole with H-slot for UHF RFID applications", In EE Congress (iEECON), 2014 International.
Yejun, et al., "A new UHF anti-metal RFID tag antenna design with open-circuited stub feed", In ICC, 2013 IEEE International conference.
Genovesi, et al., "Low-profile three-arm folded dipole antenna for UHF band RFID tags mountable on metallic Objects", Antennas and Wireless Propagation Letters, IEEE. vol. 9, 2010.
Abdulhadi, et al., "Passive UHF RFID printed monopole tag antenna for identification of metallic objects", in Antennas and Propagation Society International Symposium, 2012, IEEE.
XNP.Semiconductors, Smart label and tag ICs (UCODE) SL3S1203_1213 Datasheet, vol. rev 4.3, Nov. 27, 2013.
S. R. Best, "The significance of ground-plane size and antenna location in establishing the performance of ground-plane-dependent antennas", Antennas and propagation magazine, IEEE. vol. 15, 2009.
L. J. Chu, "Physical limitations of antenna Q" Journal of applied physics, Dec. 1948.
Rojas-Nastrucci, et al., "A study on 3D-printed coplanar waveguide with meshed and finite ground planes", in Wireless and Microwave Technology conference (WAMICON), 2014, IEEE 15th annual.
Strauss, et al., "Read range measurements of UHF RFID transponders in mobile anechoic chamber", in RFID, 2009 IEEE International conference, 2009.

* cited by examiner

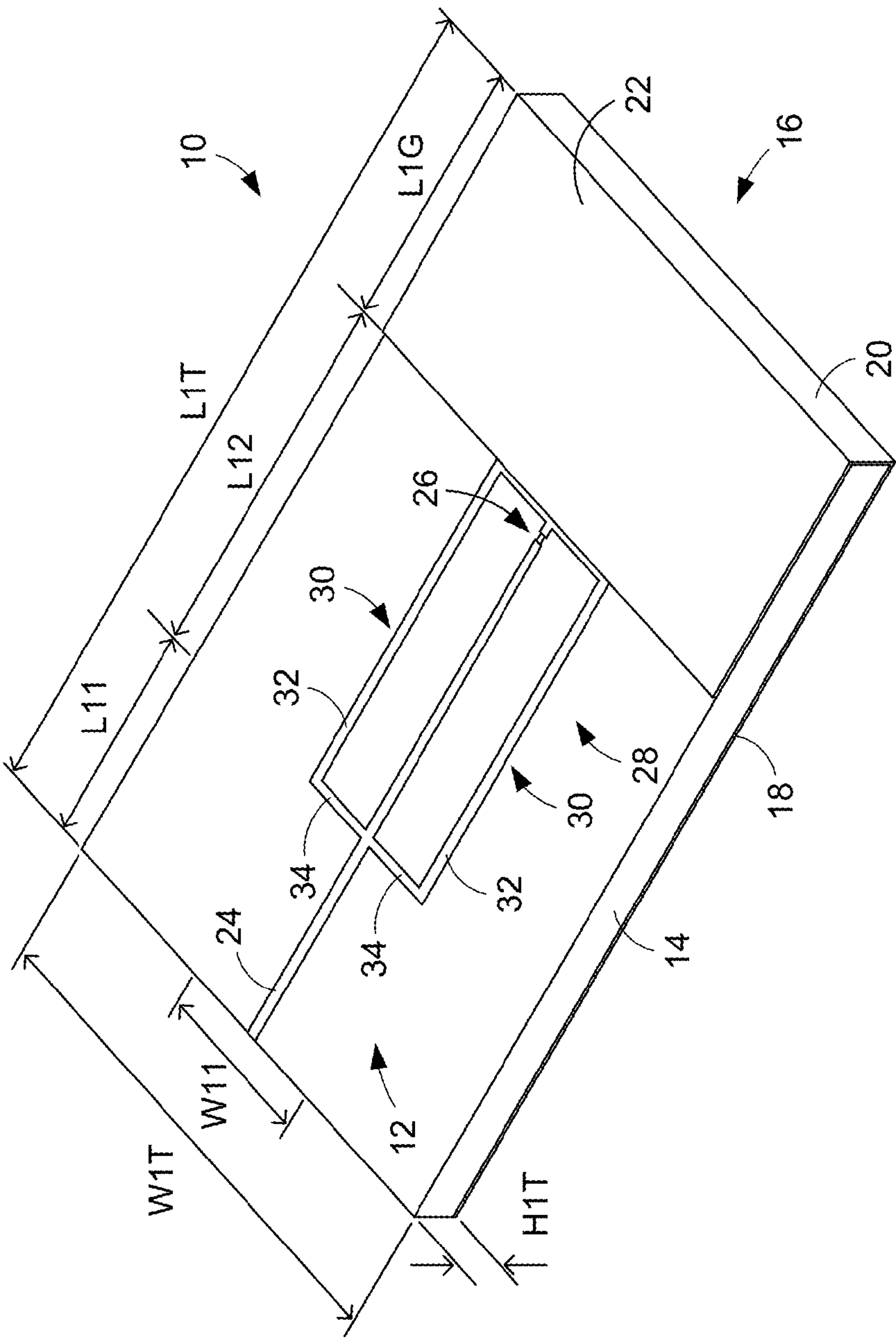


FIG. 1A

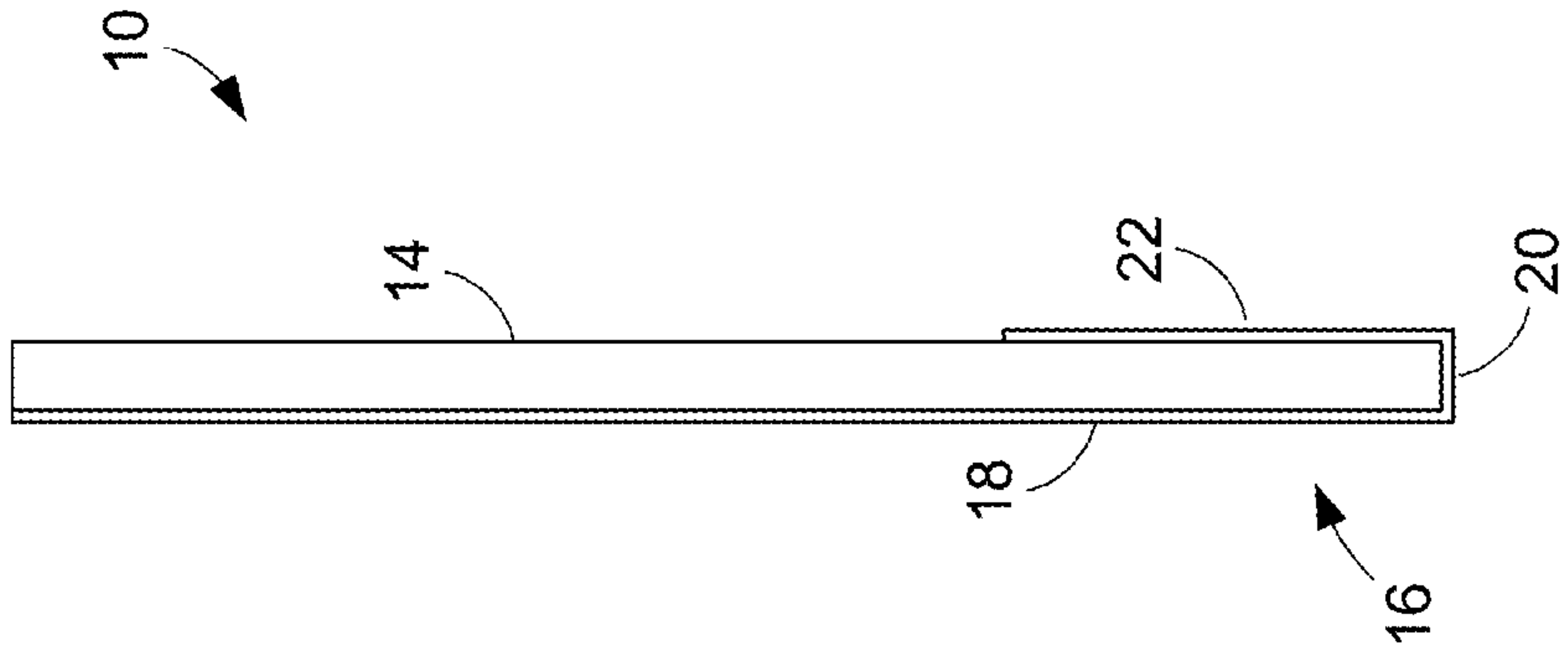
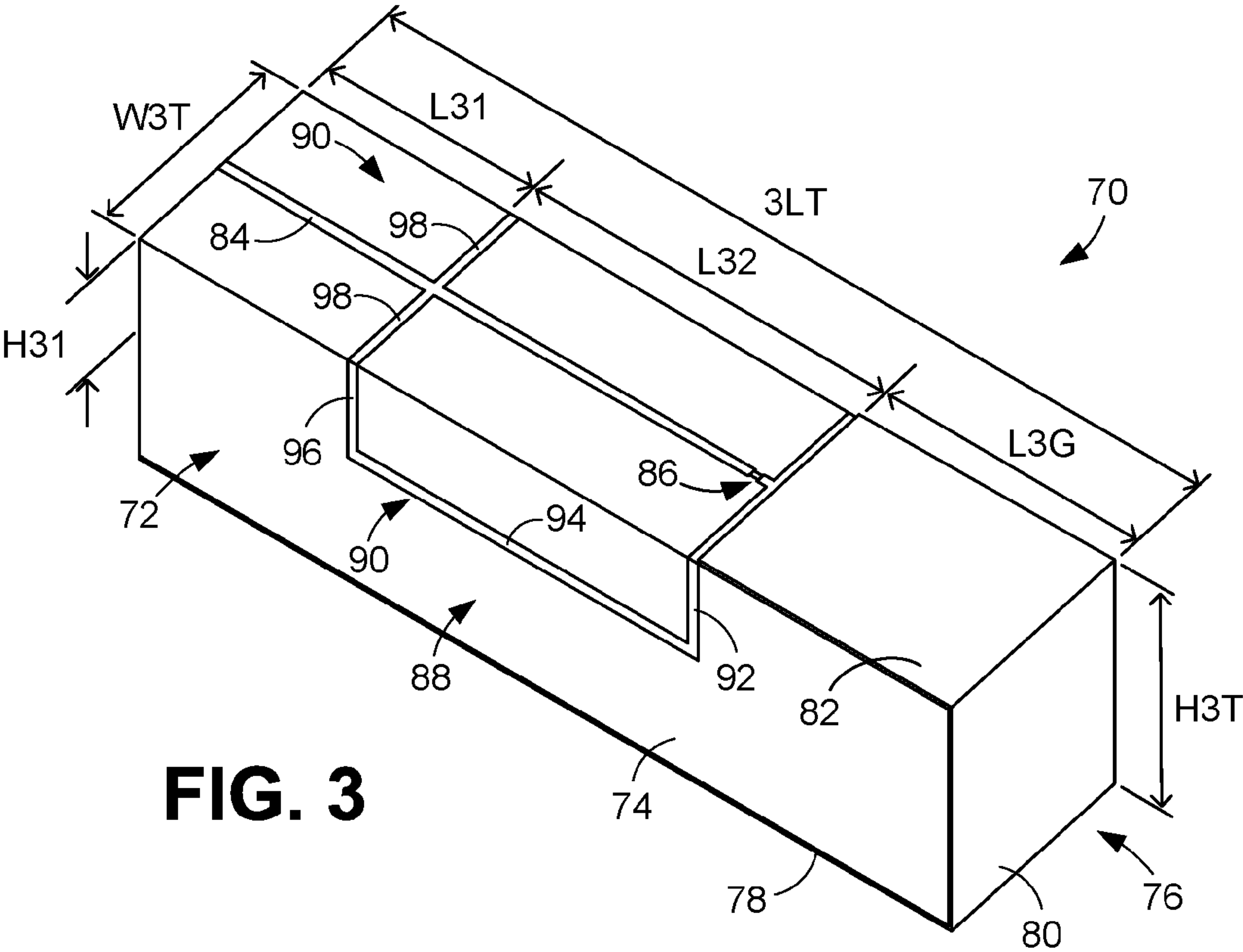
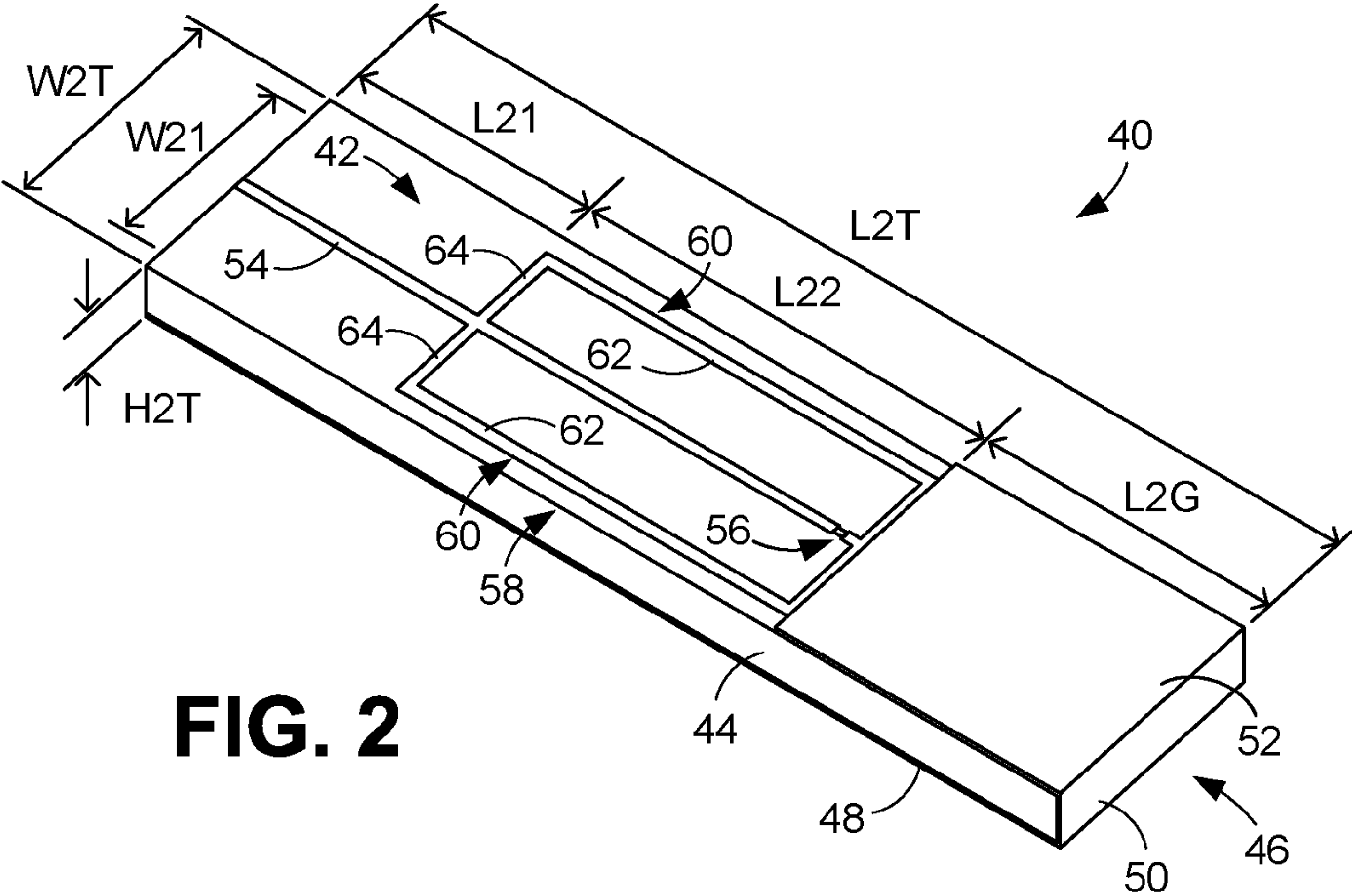


FIG. 1B



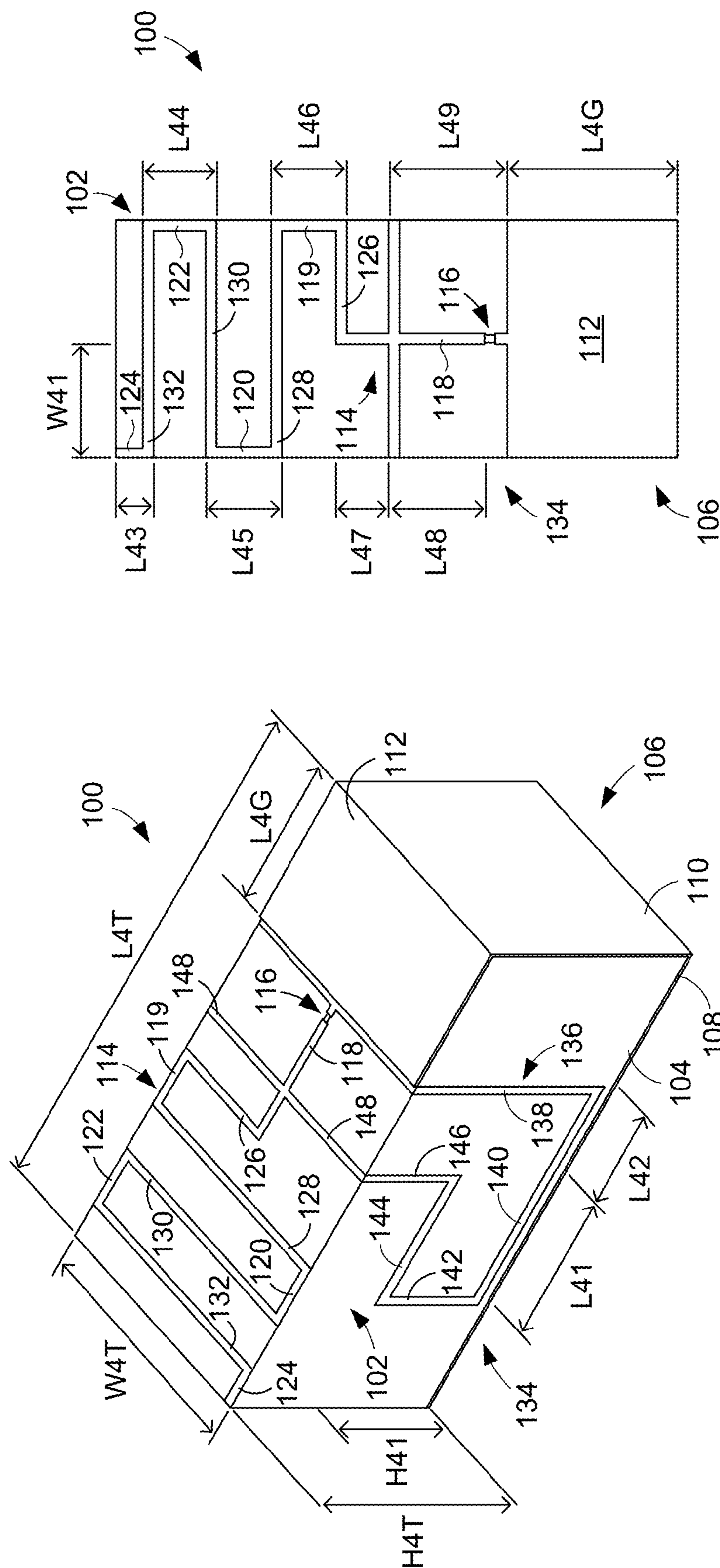


FIG. 4B

FIG. 4A

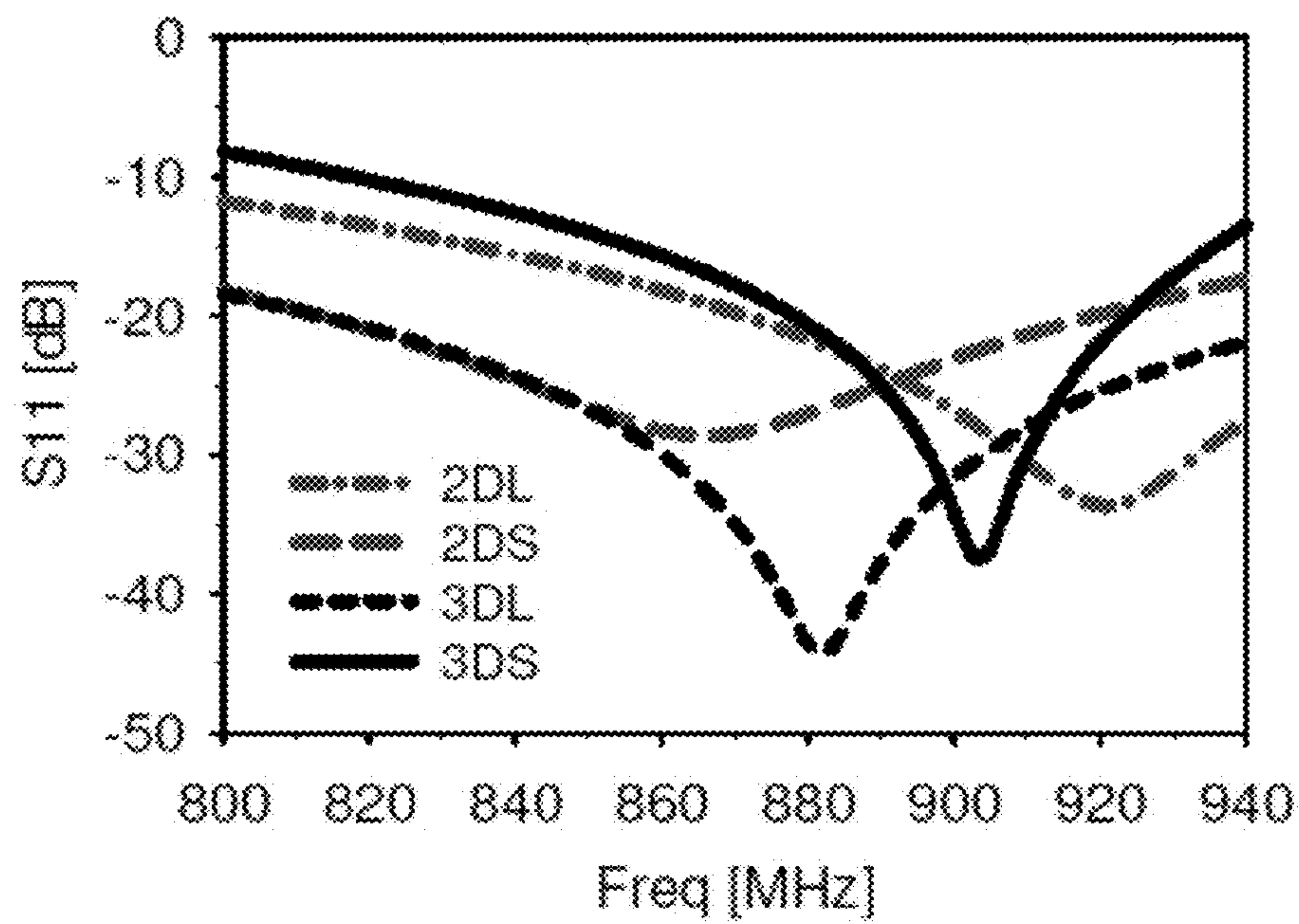


FIG. 5

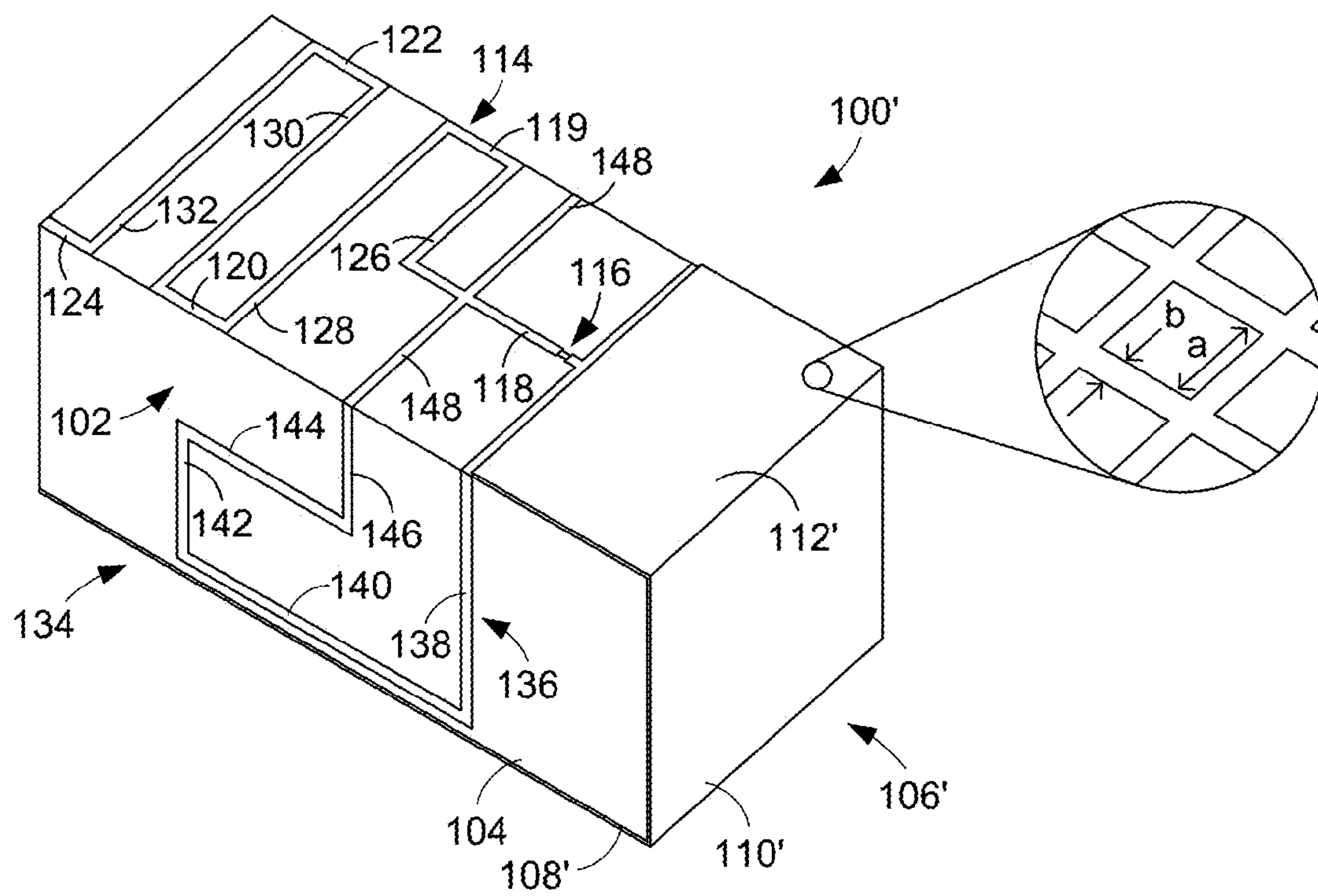


FIG. 6A

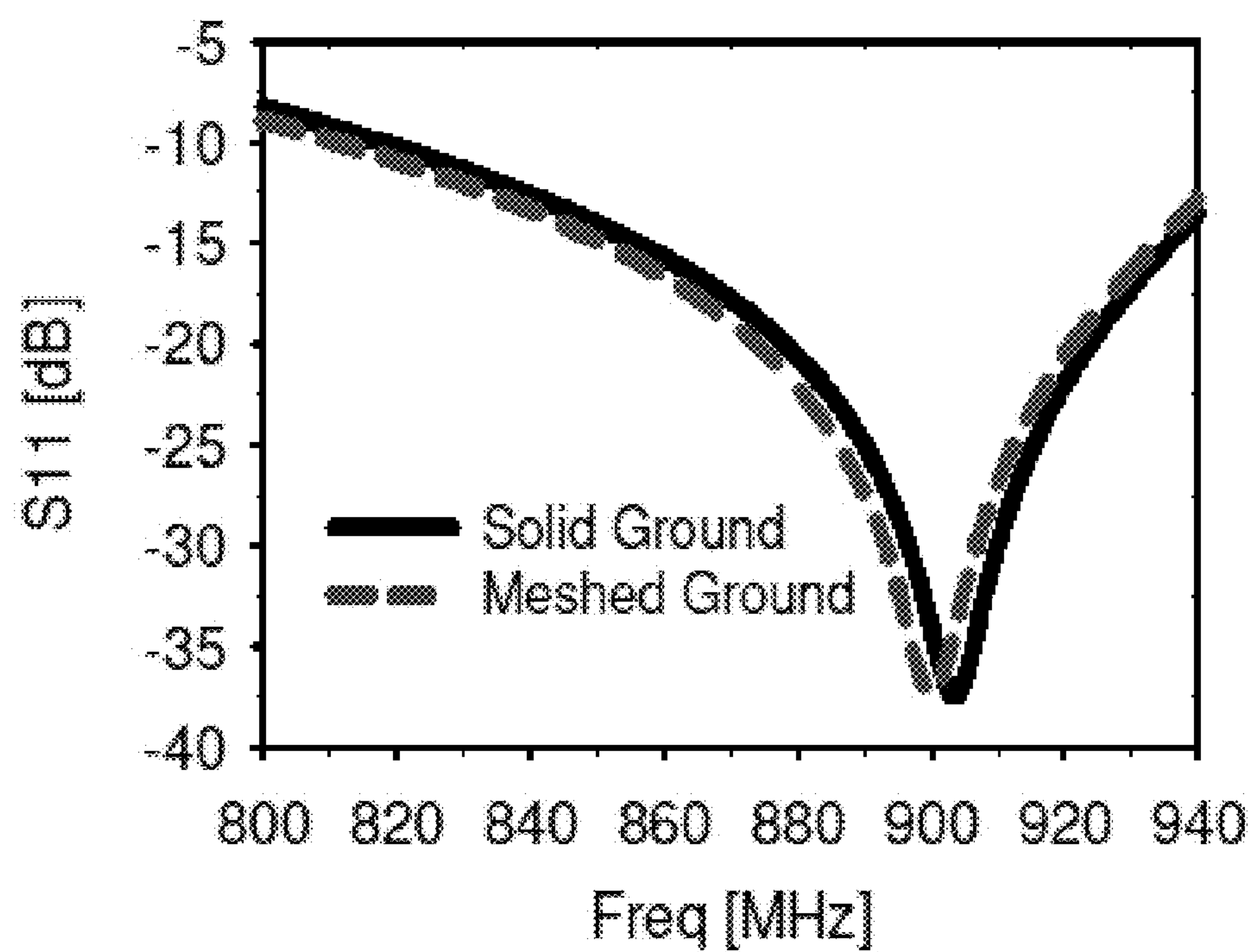


FIG. 6B

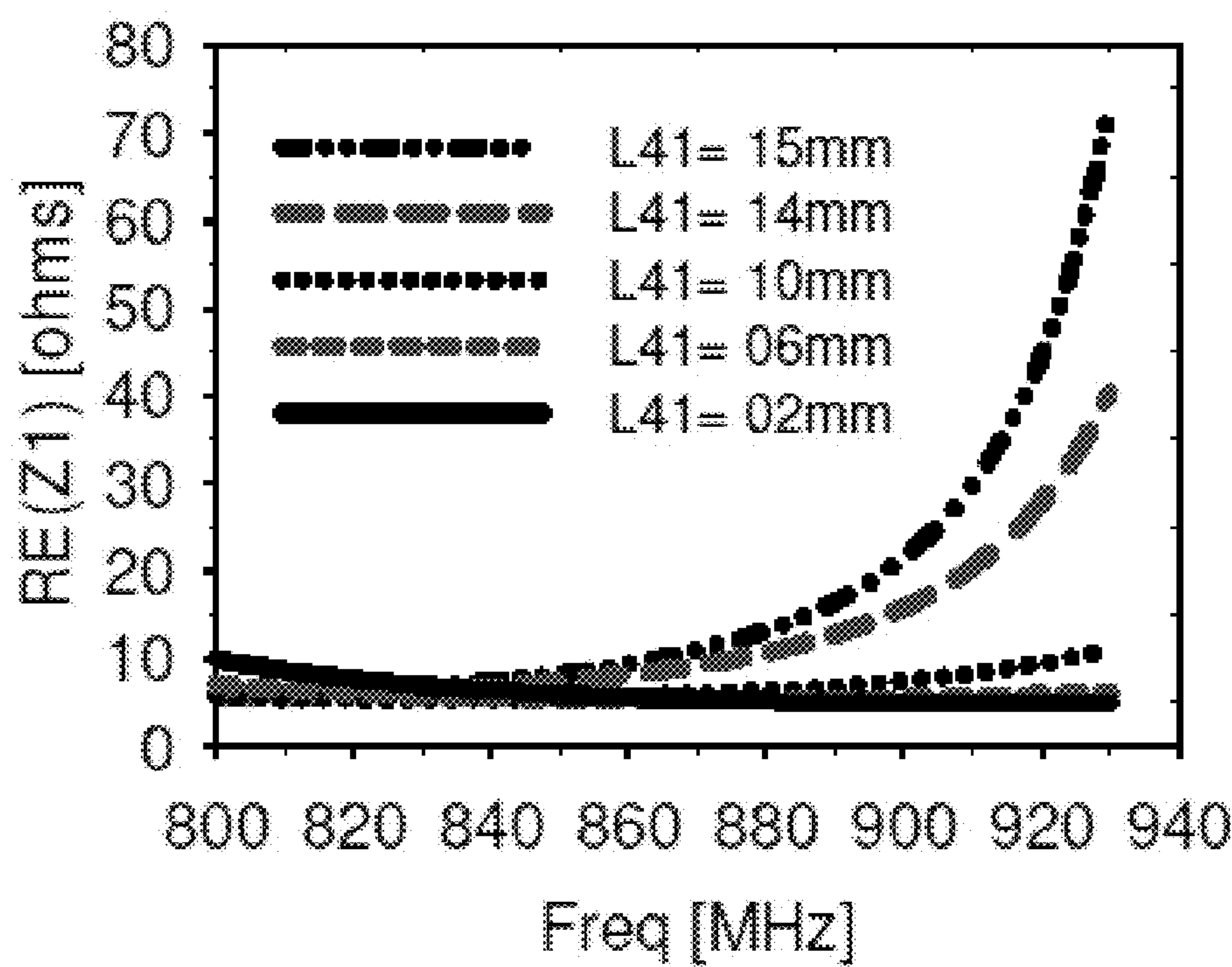


FIG. 7A

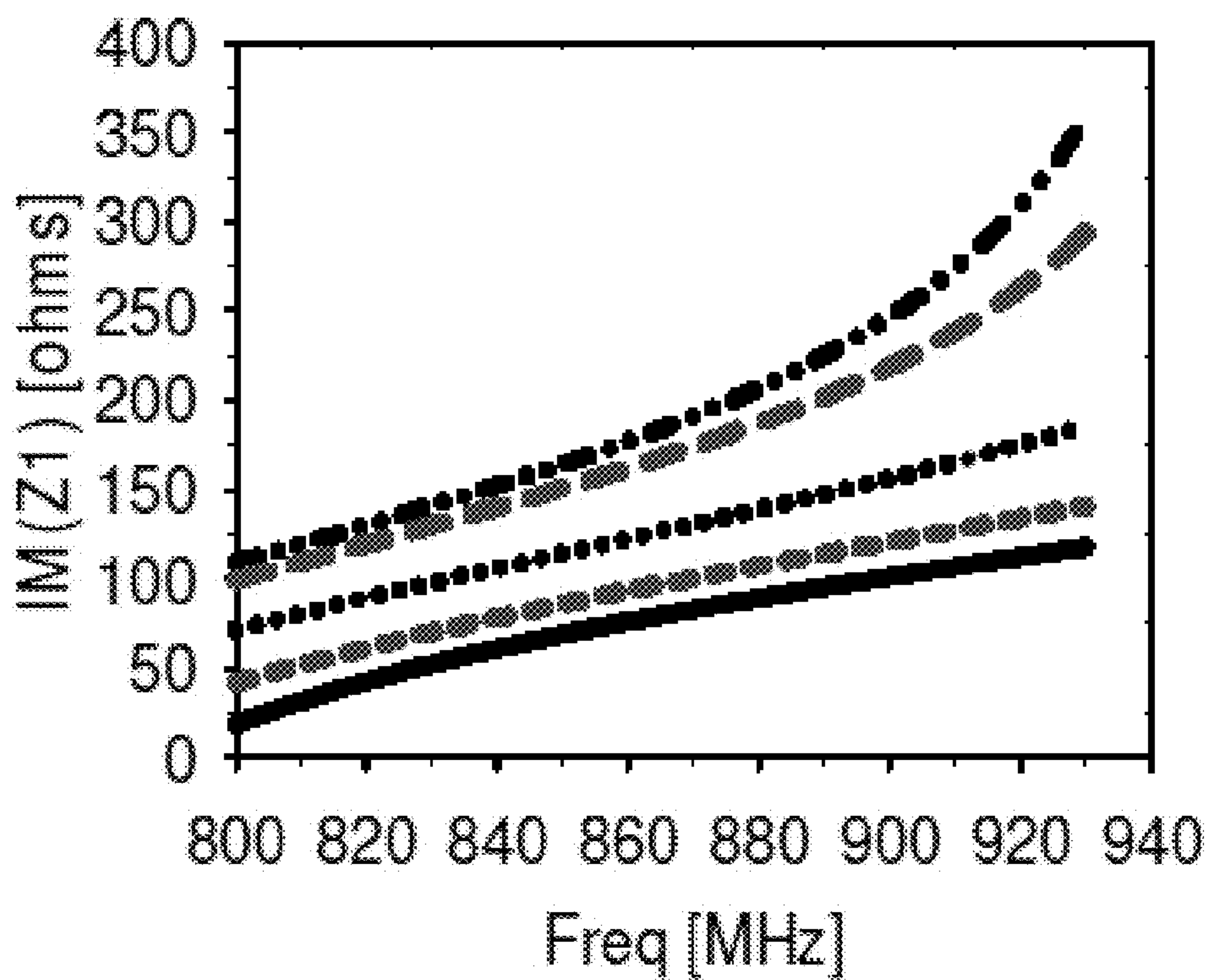


FIG. 7B

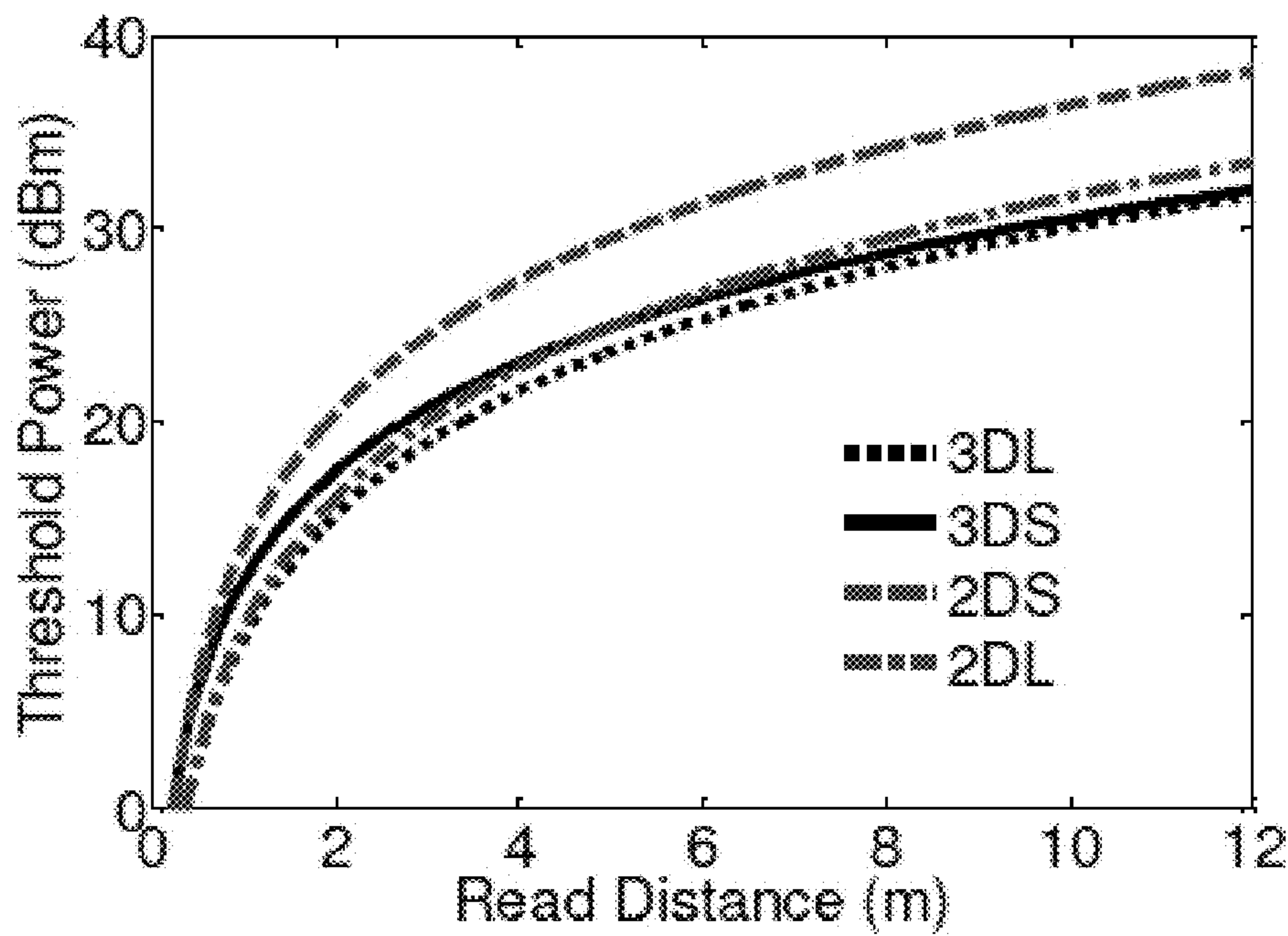


FIG. 8A

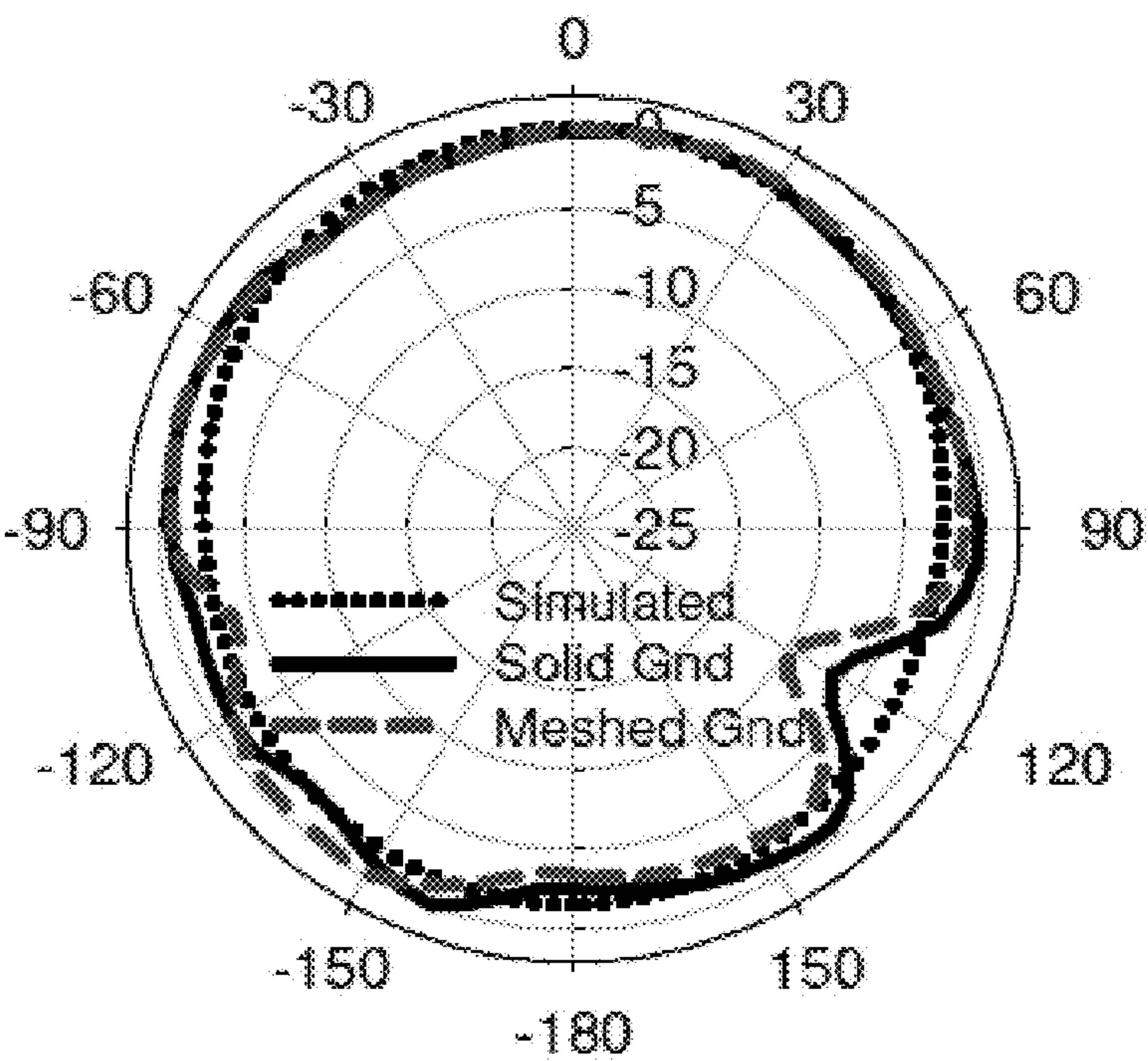


FIG. 8B

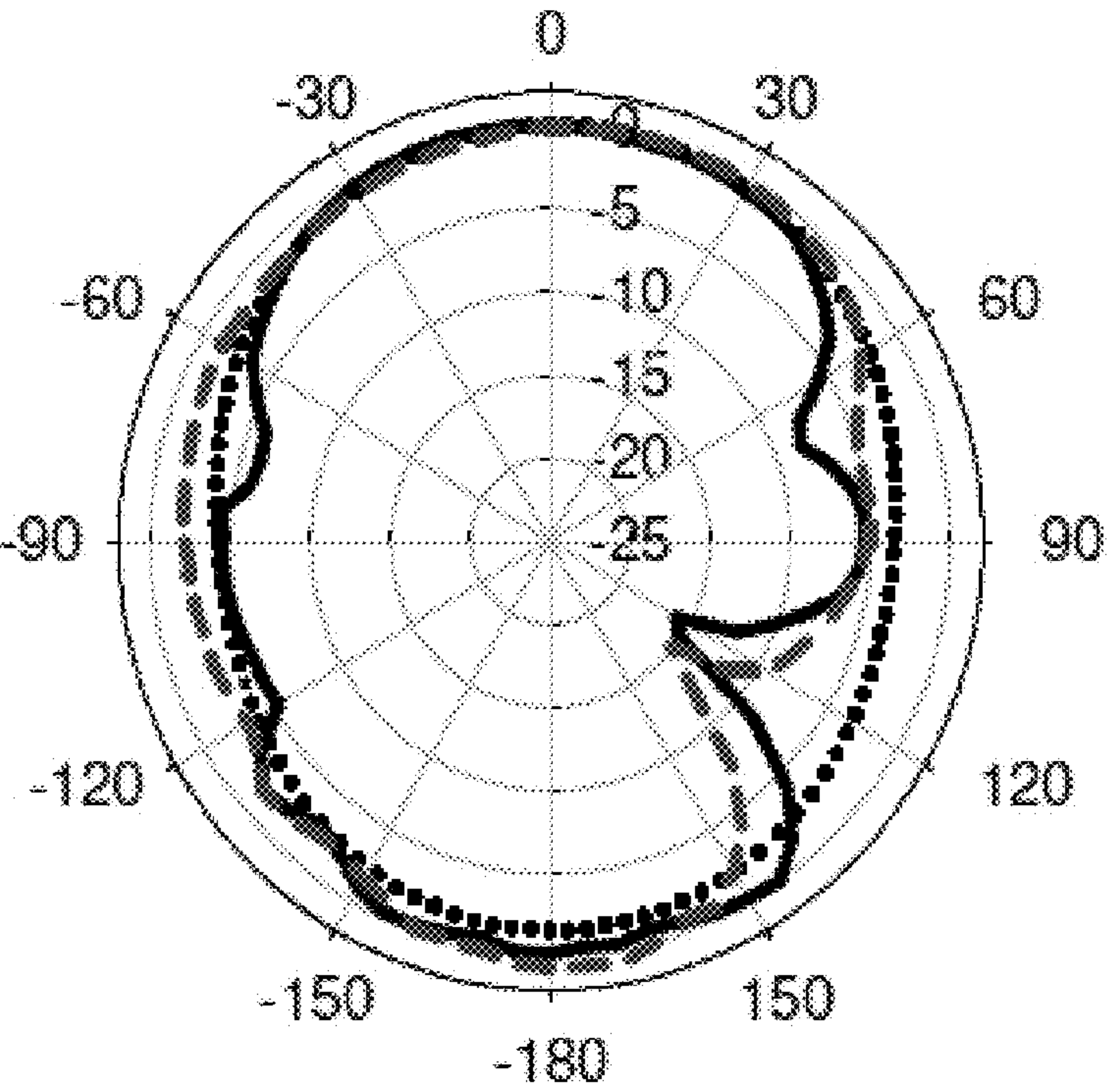


FIG. 8C

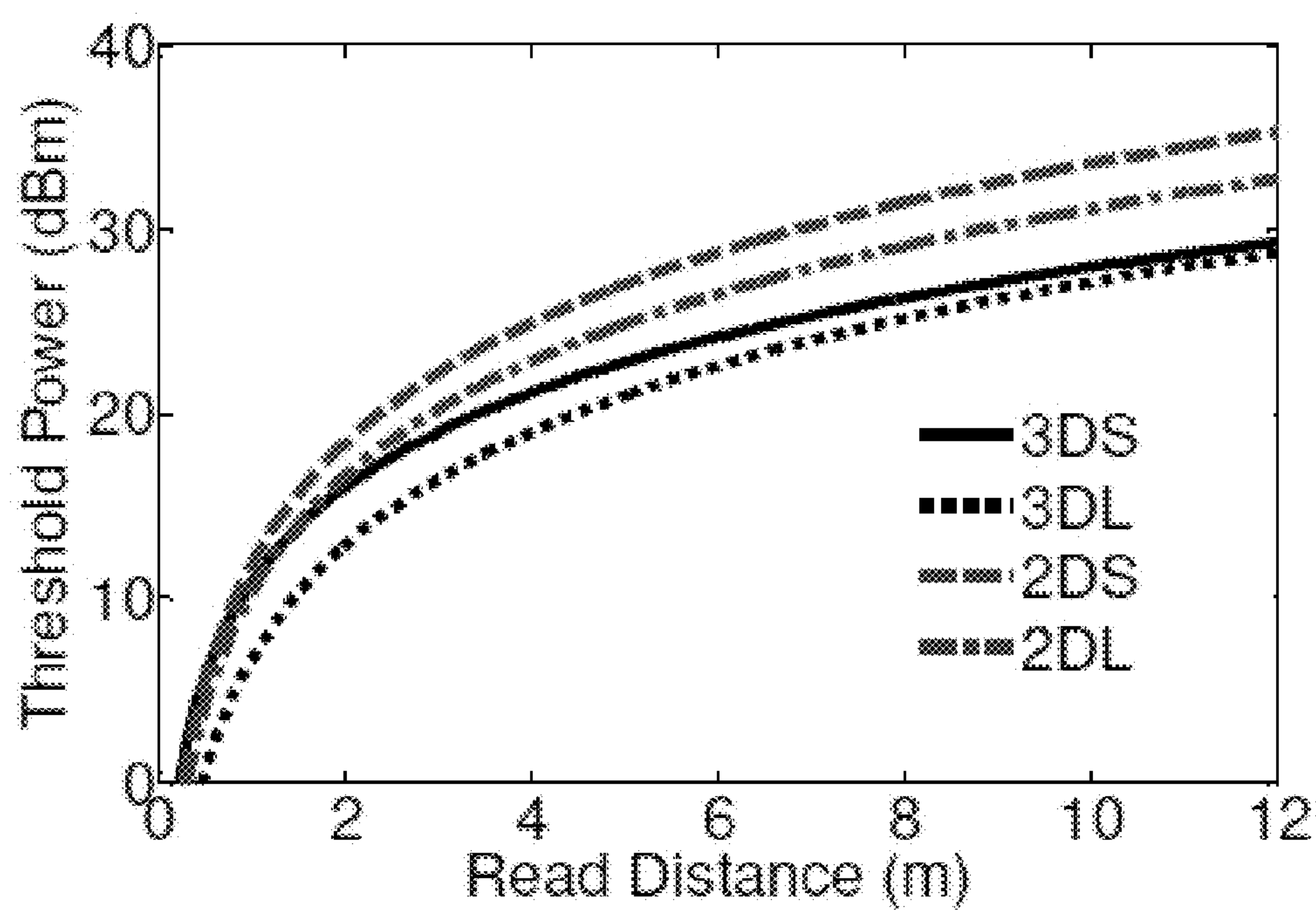


FIG. 9A

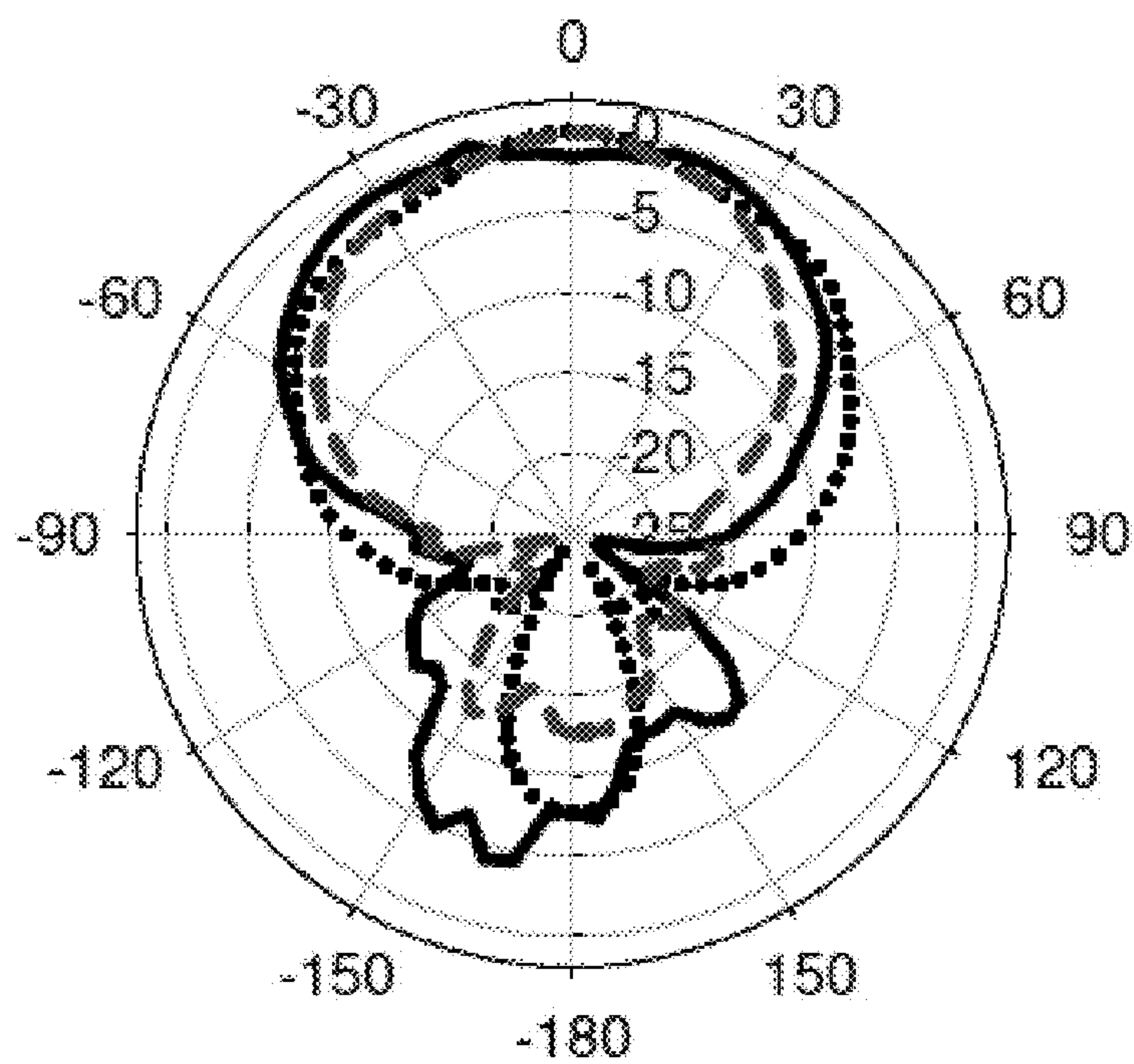
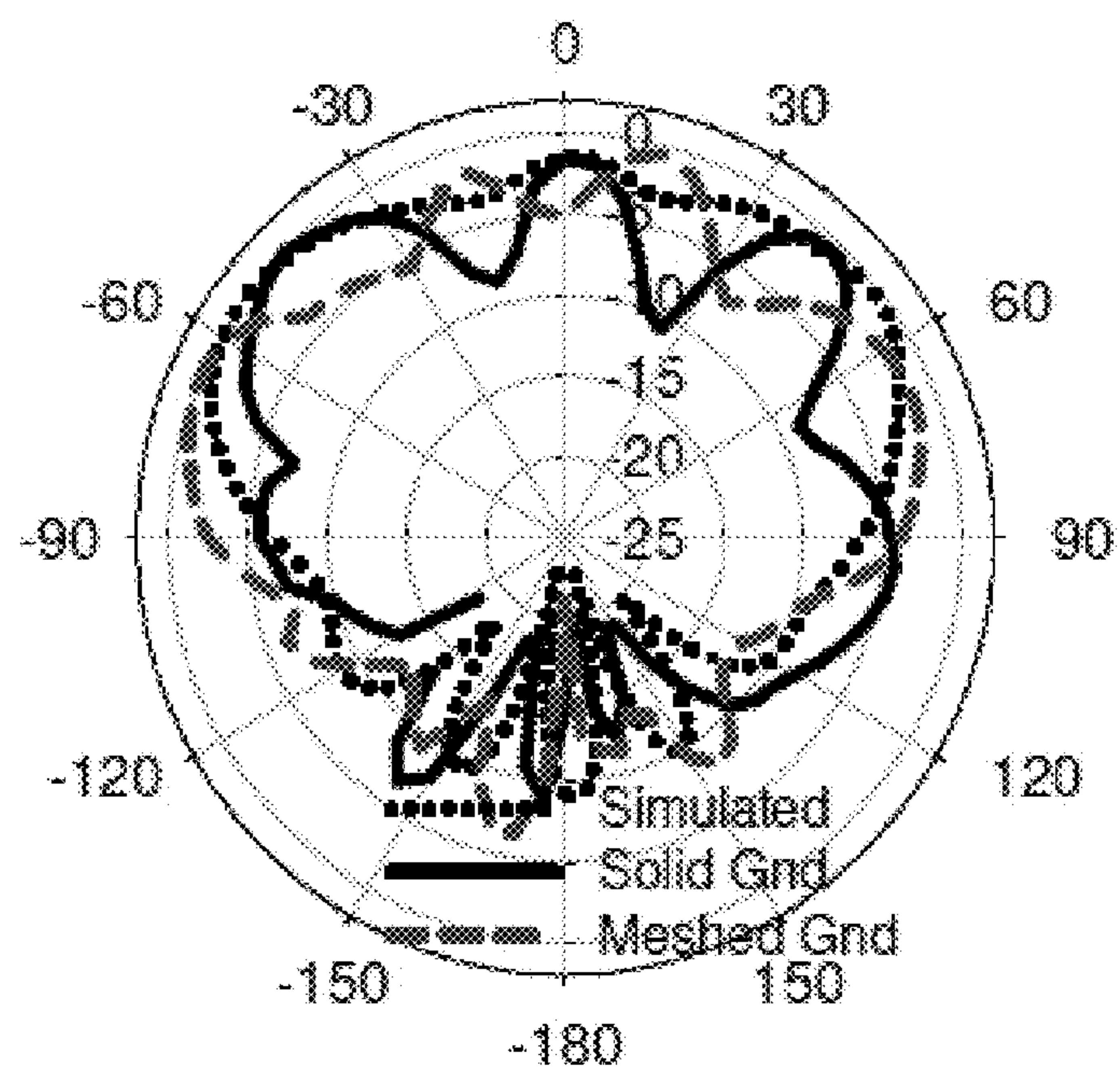


FIG. 9B

**FIG. 9C**

1

RFID TAGS FOR ON- AND OFF-METAL APPLICATIONS

BACKGROUND

Radio-frequency identification (RFID) applications continue to increase in number and new uses of the technology have prompted innovative tag designs. Achieving smaller tag footprints is of particular importance, motivating the development of three-dimensional designs that make more efficient use of the antenna volume. However, most commercial tag designs are optimized either for on-metal or off-metal conditions, and their performance is greatly diminished when the surrounding environment differs from the intended one. For example, dipole antennas can be used for off-metal systems, but often fail to operate properly when mounted horizontally over or near metallic objects. Patch antennas and folded dipoles, on the other hand, have been implemented for on-metal systems, but generally have a low off-metal read range.

From the above discussion, it can be appreciated that it would be desirable to have an RFID tag, and a tag antenna, that can be used in both on- and off-metal applications.

BRIEF DESCRIPTION OF THE DRAWINGS

The present disclosure may be better understood with reference to the following figures. Matching reference numerals designate corresponding parts throughout the figures, which are not necessarily drawn to scale.

FIG. 1A is a perspective view of a first embodiment of a radio frequency identification (RFID) tag.

FIG. 1B is a side view of the tag of FIG. 1A.

FIG. 2 is a perspective view of a second embodiment of an RFID tag.

FIG. 3 is a perspective view of a third embodiment of an RFID tag.

FIG. 4A is a perspective view of a fourth embodiment of an RFID tag.

FIG. 4B is a top view of the tag of FIG. 4A.

FIG. 5 is a graph that plots simulated reflection coefficient for the tag designs of FIGS. 1-4.

FIG. 6A is a perspective view of an RFID tag having a meshed ground plane.

FIG. 6B is a graph that plots simulated reflection coefficient for the tag design of FIG. 6A.

FIGS. 7A and 7B are graphs that show the simulated input impedance for the tag of FIG. 4 including the real part (FIG. 7A) and the imaginary part (FIG. 7B).

FIG. 8A is a graph that provides an off-metal read distance comparison for the tag designs of FIGS. 1-4.

FIGS. 8A and 8B are plots of the off-metal 10 dB normalized radiation patterns in the E-plane (FIG. 8B) and the H-plane (FIG. 8C).

FIG. 9A is a graph that provides an on-metal read distance comparison for the tag designs of FIGS. 1-4.

FIGS. 9A and 9B are plots of the on-metal 10 dB normalized radiation patterns in the E-plane (FIG. 9B) and the H-plane (FIG. 9C).

DETAILED DESCRIPTION

As described above, it would be desirable to have a radio-frequency identification (RFID) tag that incorporates an antenna that can be used in both on- and off-metal applications. Disclosed herein are RFID tags that are suitable for on-metal and off-metal applications. In some

2

embodiments, the tag comprises a passive RFID IC chip that is mounted to a top surface of a substrate, a monopole antenna that includes a radiating arm that extends out from the chip along the top surface and a matching loop having two grounded matching stubs that surround the chip and a portion of the radiating arm, and a ground plane that extends from a bottom surface of the substrate and up onto the top surface of the substrate. In some embodiments, the radiating arm is linear. In other embodiments, the radiating arm is meandered. In some embodiments, the matching loop is contained on the top surface of the substrate. In other embodiments, the matching loop further extends onto lateral surfaces of the substrate.

In the following disclosure, various specific embodiments are described. It is to be understood that those embodiments are example implementations of the disclosed inventions and that alternative embodiments are possible. All such embodiments are intended to fall within the scope of this disclosure.

Disclosed herein are RFID tags that are optimized to operate in both on-metal and off-metal conditions. Impedance matching to the passive RFID integrated circuit (IC) chip is achieved using two parallel stubs to ground, which enables the tags to cover the ISM RFID UHF bands (864-868 MHz and 902-928 MHz). On-metal read ranges of greater than 12 m are achievable using a tag having a very small footprint due to its three-dimensional design. Meshed ground planes can be used to reduce the conductive ink usage (by ~50%) and printing time, while having minimal effect on the tag performance.

FIGS. 1A and 1B illustrate a first embodiment of an RFID tag 10. In this embodiment, the tag 10 comprises a two-dimensional antenna 12 that is formed on a low-permittivity substrate 14. The substrate 14 can be formed as a rectangular cuboid having a top surface, a bottom surface, opposed end surfaces, and opposed lateral surfaces. In some embodiments, the substrate 14 comprises an acrylonitrile butadiene styrene (ABS) substrate formed using an additive manufacturing method, such as fused deposition modeling (FDM). In some embodiments, the thickness of the substrate 14 is many times smaller than the length of the substrate. By way of example, the substrate 14 can be 6 mm thick and have an area of approximately 13,126.5 mm². In some embodiments, the measured electrical properties at 1 GHz of the substrate 14 are $\epsilon_r=2.6$ and $\tan \delta=0.0058$.

The design of the tag 10 enables constructive, in-phase reflections from a ground plane 16 that extends along the bottom of the substrate 14 and wraps around an end of the substrate to extend across a portion of the top of the substrate. Accordingly, the ground plane 16 comprises a lower portion 18 that covers a bottom surface of the substrate 14, an end portion 20 that covers an end surface of the substrate, and a top portion 22 that covers a portion of a top surface of the substrate on which the antenna 12 is formed.

The antenna 12 is configured as a planar monopole antenna comprising a linear radiating arm 24 that is used as the radiating element and achieves broadside radiation particularly while mounted on metallic objects. This arm 24 extends along a longitudinal direction of the substrate 14 from a passive RFID integrated circuit (IC) chip 26. By way of example, the RFID IC chip 26 comprises an NXP UCODE G2i1 SL3S1203_1213 passive RFID IC chip, which has a sensitivity of -18 dBm. In some embodiments, the arm 24 is formed by micro-dispensing of silver paste, such as Dupont CB028 silver paste, on the top surface of the substrate 14. The paste can be printed using, for example, an nScrypt Tabletop 3Dn printer having a 125 μ m inner diam-

eter ceramic tip. Once the paste has been printed, it can be dried. For example, the paste can be dried at 90° C. for 60 minutes. A monopole design was also chosen because of its ease of manufacturing and integration with printed circuit boards and surface-mount components, such as the chip 26.

The antenna 12 is designed to be conjugate matched to the RFID IC chip 26, which can have normal mode impedances at 866 MHz and 915 MHz of $Z_{in}=(25-j237) \Omega$ and $Z_{in}=(23-j224) \Omega$, respectively. The stable impedance over frequency makes the chip useful for dual band operation. The impedance matching from the antenna 12 to the RFID IC chip 26 is achieved using a matching loop 28 including two grounded tuning stubs 30. The stubs 30 each include a longitudinal segment 32 that extends from the top portion 22 of the ground plane 16 along the longitudinal direction of the substrate 14 on either side of the radiating arm 24 (parallel thereto), and a transverse segment 34 that extends from an end of the longitudinal segment along a transverse direction of the substrate to the radiating arm. The lengths of the longitudinal and transverse segments 32, 34 of the stubs 30 can be adjusted to provide the necessary susceptance to achieve a matched condition. A simulated broadside gain of 3.16 dBi is achieved both on- and off-metal.

Example dimensions for the RFID tag 10 are shown in Table I. In this embodiment, the antenna's radiating arm 12 is 67.5 mm long and is optimized from a $\lambda_g/4$ length at the center frequency of the European (862-868 MHz) and American (902-928 MHz) ISM RFID bands.

TABLE I

Dimensions for the Tag Designs	
Variable	Value (mm)
LIT	98.75
L11	25.50
L12	42.00
L1G	31.25
WIT	57.00
W11	19.00
HIT	06.00
L2T	98.75
L21	25.50
L22	42.00
L2G	31.25
W2T	22.50
W21	19.00
H2T	06.00
L3T	97.75
L31	40.50
L32	26.25
L3G	31.00
W3T	22.50
H3T	22.00
H31	10.75
W41	10.25
L4T	52.75
L41	14.00
L42	12.00
L43	03.50
L44	07.00
L45	07.00
L46	07.00
L47	05.00
L48	09.00
L49	11.25
L4G	16.00
H4T	22.00
H41	10.75
W4T	22.50

FIG. 2 illustrates a second embodiment of an RFID tag 40 that is similar in design to the RFID tag 10. Accordingly, the

tag 40 also comprises a two-dimensional antenna 42 that is formed on a low-permittivity substrate 44, which can be 6 mm thick and made of ABS.

The tag 40 includes a ground plane 46 that comprises a lower portion 48 that covers a bottom surface of the substrate 44, an end portion 50 that covers an end surface of the substrate, and a top portion 52 that covers a portion of a top surface of the substrate on which the antenna 42 is formed.

The antenna 42 is configured as a planar monopole antenna including a linear radiating arm 54 that extends along a longitudinal direction of the substrate 44 from a passive RFID integrated circuit (IC) chip 56. As with the arm 24, the arm 54 can be formed by micro-dispensing of silver paste on the top surface of the substrate 44.

The antenna 42 further comprises a matching loop 58 including two grounded tuning stubs 60, which each include a longitudinal segment 62 that extends from the top portion 52 of the ground plane 46 along the longitudinal direction of the substrate 44 on either side of the radiating arm 54 (parallel thereto), and a transverse segment 64 that extends from an end of the longitudinal segment along a transverse direction of the substrate to the radiating arm.

While the embodiment of FIG. 2 shares many similarities with the embodiment of FIG. 1, the RFID tag 40 shown in FIG. 2 is much smaller than the RFID tag 10 shown in FIG. 1. In particular, the tag 40 is much narrower than the tag 10 and, therefore, has a smaller footprint. In some embodiments, the tag 40 has a width of 22.5 mm, as compared to 57 mm for the tag 10, and an area of 5,898.7 mm², which reflects a footprint reduction of 222%. Although the tag 40 has a smaller footprint, it is designed to provide similar performance for both on- and off-metal applications. The reduction of the ground plane width, however, compromises the antenna radiation efficiency and therefore the peak broadside gain due to an increase in edge radiation. The simulated off-metal broadside gain for the tag 40 design is 1.8 dBi compared to 3.16 dBi for the tag 10.

Example dimensions for the RFID tag 40 are also shown in Table I.

One approach to account for the gain reduction of the smaller ground plane is to introduce a three-dimensional geometry. FIG. 3 illustrates an embodiment of an RFID tag 70 that has such a geometry. The tag 70 comprises a three-dimensional antenna 72 that is formed on a thick, low-permittivity substrate 74, which can be made of ABS. In some embodiments, the thickness of the substrate 74 is approximately one-quarter the length of the substrate. By way of example, the substrate 74 can be approximately 1 mm thick.

The tag 70 includes a ground plane 76 that comprises a lower portion 78 that covers a bottom surface of the substrate 74, an end portion 80 that covers an end surface of the substrate, and a top portion 82 that covers a portion of a top surface of the substrate on which the antenna 72 is formed.

The antenna 72 is configured as a planar monopole antenna including a linear radiating arm 84 that extends along a longitudinal direction of the substrate 74 from a passive RFID integrated circuit (IC) chip 86. The arm 84 can be formed by micro-dispensing of silver paste on the top surface of the substrate 74.

The antenna 72 further comprises a matching loop 88 that includes two grounded tuning stubs 90. In this embodiment, however, the stubs 90 extend across the top surface of the substrate 74 and opposed lateral surfaces of the substrate. More particularly, the stubs 90 include a first vertical segment 92 that extends downward from the top surface and the top portion 82 of the ground plane 76 along the lateral

5

surface of the substrate **74**, a horizontal segment **94** that extends from an end of the first vertical segment along the lateral surface and along the longitudinal direction of the substrate, a second vertical segment **96** that extends upward from an end of the horizontal segment along the lateral surface of the substrate to its top surface, and a transverse segment **98** that extends from an end of the second vertical segment along the top of the substrate in the transverse direction to the radiating arm **84**. With this configuration, a much larger matching loop **88** is provided without increasing the footprint of the tag **70**.

Example dimensions for the RFID tag **70** are also shown in Table I.

Further size reduction can be achieved by using a meandered radiating arm to compress the antenna into a reduced footprint. FIGS. **4A** and **4B** illustrate an embodiment of an RFID tag **100** that utilizes such a configuration. The tag **100** also comprises a three-dimensional antenna **102** that is formed on a thick, low-permittivity substrate **104** that can be made of ABS. In some embodiments, the thickness of the substrate **104** is approximately half the length of the substrate. By way of example, the substrate **104** is approximately 1 mm thick.

The tag **100** includes a ground plane **106** that comprises a lower portion **108** that covers a bottom surface of the substrate **104**, an end portion **110** that covers an end surface of the substrate, and a top portion **112** that covers a portion of a top surface of the substrate on which the antenna **102** is formed.

The antenna **102** is configured as a planar monopole antenna including a meandered radiating arm **114** that extends along a longitudinal direction of the substrate **104** from a passive RFID integrated circuit (IC) chip **116**. As shown in FIGS. **4A** and **4B**, the arm **114** includes multiple longitudinal segments **118**, **119**, **120**, **122**, and **124** that connect with multiple transverse segments **126**, **128**, **130**, and **132** to form a continuous meandered structure that results in a relatively long radiating arm **114** that occupies a relatively small area. The longer radiating arm **114** is needed to overcome the reduction in effective length that is produced by greater electric field coupling between the segments. As before, the arm **114** can be formed by micro-dispensing of silver paste on the top surface of the substrate **104**.

The antenna **102** further comprises a matching loop **134** that includes two grounded tuning stubs **136** that extend across the top and lateral surfaces of the substrate **104**. More particularly, the stubs **136** include a first vertical segment **138** that extends downward from the top surface and the top portion **112** of the ground plane **106** along the lateral surface of the substrate **104**, a first horizontal segment **140** that extends from an end of the first vertical segment along the lateral surface and along the longitudinal direction of the substrate, a second vertical segment **142** that extends upward from an end of the first horizontal segment along the lateral surface of the substrate, a second horizontal segment **144** that extends from an end of the second vertical segment along the lateral surface and along the longitudinal direction of the substrate, a third vertical segment **146** that extends upward from an end of the second horizontal segment along the lateral surface of the substrate to its top surface, and a transverse segment **148** that extends from an end of the third vertical segment along the top of the substrate in the transverse direction to the radiating arm **114**.

The geometry of the tag **100** takes advantage of the available radiation sphere in a more efficient way when compared with the other designs and provides an electrical

6

size at 915 MHz of $ka=0.588$ compared to 1.093 (tag **10**), 0.972 (tag **40**) and 0.983 (tag **70**).

Example dimensions for the RFID tag **100** are also shown in Table I.

FIG. **5** shows the simulated reflection coefficients for the RFID tags described above. The tag **100** enables an area reduction compared to the tag **10** of 520% while maintaining a similar on-metal performance with a broadside simulated gain of 5.02 dBi while mounted over a 0.9 m diameter copper disc and 3 dBi gain while mounted over a 300×300 mm² rectangular ground plane. The four tags show a simulated -10 dB reflection coefficient bandwidth that allows them to operate in both the European and American RFID ISM frequency bands. Simulations were performed with ANSYS HFSS 15.

If desired, the amount of conductive paste and the printing time can be reduced when fabricating the RFID tags. FIG. **6A** illustrates an example of this. In this embodiment, the paste used to form the ground plane **106'** of the RFID tag **100'** was reduced by using a meshed configuration instead of a solid one (the ground plane **106'** includes a lower portion **108'**, an end portion **110'**, and a top portion **112'**). The ground density (D) defines the ratio of the conductor used with the meshed ground to the conductor needed for a solid ground. If the mesh dimensions are selected as $a=0.45$ mm and $b=0.45$ mm (as illustrated in FIG. **6A**) the ground density is 51.5%, which means that approximately half as much ink is needed to fabricate the ground plane. FIG. **6B** shows the simulated return loss (referenced to the chip impedance) when using a meshed configuration.

Impedance tuning of the FIG. **4** design to accommodate different ICs or operating frequencies can be accomplished by manipulating the length of the tuning stubs during the initial design stage. In the embodiment of FIG. **4**, the tuning stubs are connected to ground and wrapped around the lateral surface before making contact with the radiating arm. The length **L41** can be easily adjusted on both stubs to fine tune the antenna's reactance, and consequently the resonant frequency. FIGS. **7A** and **7B** show the changes in the antenna input impedance for different **L41** values.

RFID tags having the above configurations were fabricated and tested, and their performance was evaluated. Radiation pattern measurements were made inside an anechoic chamber. Read range measurements were performed using a movable fixture to manually adjust the distance. A CS101 Handheld RFID reader was used to determine read range for each tag. The distance was measured with a BOSCH GLM15 laser measurement tool. The reader power setting (threshold power) was increased from 10 dBm up to 31 dBm and plotted against maximum read distance. The measured data was fitted with a model consistent with the Friis equation: $\log_{10}(1/d^2)$, where d is the distance between the reader and the tag.

FIG. **8A** shows the measured off-metal threshold power against maximum read distance. For 31 dBm threshold power, the FIG. **3** and FIG. **4** designs reached a read distance of approximately 11 m, which is almost 2 meters better than what is obtained with the larger FIG. **1** design. FIGS. **8B** and **8C** show the simulated and measured E-plane and H-plane normalized gain patterns, respectively.

On-metal measurements were performed with the tags placed on a 300×300 mm² copper plane. FIG. **9A** shows the measured threshold power against maximum read distance. For 31 dBm threshold power, the FIG. **3** and FIG. **4** designs reached a read distance of approximately 12.5 meters, which is almost 4 meters better than what is obtained with the larger FIG. **1** design. FIGS. **9B** and **9C** show the simulated

and measured E-plane and H-plane normalized gain patterns, respectively, for the on-metal configuration.

Table II provides a comparison of measured read range of the four tag designs and several previously proposed tags.

TABLE II

Measured Read Range Comparison			
Element	Electrical Size (ka) 915 MHz	Measured Off Metal Read Range (m)	Measured On Metal Read Range (m)
2DL**	1.093	10.0	10.2
2DS**	0.972	6.5	7.9
3DL**	0.983	11.5	12.5
3DS**	0.588	11.3	12.1
AMC M [7]*	1.133	10.0	8.3
3-Arm[5]***	1.210	2.0	5.0
Patch[4]*	1.395	—	2.5
Confidex Irons. Micro*	0.369	—	5.0

Threshold power = **(1.25 W), *(4 W), ***(2 W)

As described above, multiple RFID tag antenna designs have been disclosed for dual band operation (ISM RFID UHF 864-868 MHz and 902-928 MHz). A baseline tag design (FIG. 1) shows similar on- and off-metal performance. This design was then compressed into 3 different designs having smaller footprints and improved performance. For a threshold power of 31 dBm, the maximum measured on- and off-metal read distance was 12.5 m and 11.5 m, respectively, for the FIG. 3 design, which had dimensions of 97.75×22.5×22 mm. Similar performance was obtained with a more compact design (FIG. 4) with dimensions of 52.75×22.5×22 mm and read range on- and off-metal of 12.1 m and 11.3 m, respectively. Impedance matching and tunability was obtained by using two grounded stubs, enabling functionality with multiple RFID passive ICs.

The invention claimed is:

1. A radio-frequency identification (RFID) tag comprising:
 - a substrate having a top surface including a bottom surface, opposed end surfaces, and opposed lateral surfaces;
 - a passive RFID integrated circuit (IC) chip mounted to the top surface of the substrate;
 - a monopole antenna that includes a planar radiating arm that extends out from the RFID IC chip along the top surface of the substrate and a matching loop having two grounded matching stubs that surround the chip and a portion of the radiating arm, wherein the matching loop extends across the top surface of the substrate and onto the lateral surfaces of the substrate; and
 - a ground plane formed on the bottom surface, an end surface, and the top surface of the substrate, the ground plane being electrically coupled to the matching stubs and the radiating arm.
2. The RFID tag of claim 1, wherein the substrate is made of acrylonitrile butadiene styrene.
3. The RFID tag of claim 1, wherein the substrate is a rectangular cuboid.
4. The RFID tag of claim 1, wherein a thickness of the substrate is approximately one-quarter a length of the substrate.

5. The RFID tag of claim 1, wherein a thickness of the substrate is approximately half a length of the substrate.
6. The RFID tag of claim 1, wherein the radiating arm is linear.
7. The RFID tag of claim 1, wherein the radiating arm is meandered.
8. The RFID tag of claim 1, wherein the matching loop is confined to the top surface of the substrate.
9. The RFID tag of claim 1, wherein the ground plane has a meshed configuration.
10. An antenna comprising:
 - a substrate having a top surface including a bottom surface, opposed end surfaces, and opposed lateral surfaces;
 - a monopole antenna that includes a planar radiating arm that extends along the top surface of the substrate and a matching loop having two grounded matching stubs that surround a portion of the radiating arm wherein the matching loop extends across the top surface of the substrate and onto the lateral surfaces of the substrate; and
 - a ground plane formed on the bottom surface, an end surface, and the top surface of the substrate, the ground plane being electrically coupled to the matching stubs and the radiating arm.
11. The antenna of claim 10, wherein the substrate is made of acrylonitrile butadiene styrene.
12. The antenna of claim 10, wherein a thickness of the substrate is approximately one-quarter a length of the substrate.
13. The antenna of claim 10, wherein a thickness of the substrate is approximately half a length of the substrate.
14. The antenna of claim 10, wherein the radiating arm is linear.
15. The antenna of claim 10, wherein the radiating arm is meandered.
16. The antenna of claim 10, wherein the matching loop is confined to the top surface of the substrate.
17. The antenna of claim 10, wherein the ground plane has a meshed configuration.
18. A method for fabricating a radio-frequency identification (RFID) tag, the method comprising:
 - forming a substrate using an additive manufacturing fabrication method, the substrate having a top surface bottom surface, opposed end surfaces, and opposed lateral surfaces;
 - mounting an RFID integrated circuit (IC) chip on the top surface of the substrate;
 - printing a monopole antenna on the top surface of the substrate that includes a planar radiating arm that extends from the RFID IC chip and a matching loop having two grounded matching stubs that surround the RFID IC chip and a portion of the radiating arm wherein the matching loop extends across the top surface of the substrate and onto the lateral surfaces of the substrate; and
 - printing a ground plane on the bottom surface, an end surface, and the top surface of the substrate, the ground plane being electrically coupled to the matching stubs and the radiating arm.

* * * * *